PHOTONICS Research

Terahertz wave generation from liquid nitrogen

Alexei V. Balakin,[1,2] Jean-Louis Coutaz,[3] Vladimir A. Makarov,[1,2] Igor A. Kotelnikov,[4,5] Yan Peng,[1] Peter M. Solyankin,[1,6] Yiming Zhu,[1,7] and Alexander P. Shkurinov[1,2,8]

[1]Terahertz Technology Innovation Research Institute, Shanghai Key Laboratory of Modern Optical System, Terahertz Spectrum and Imaging Technology Cooperative Innovation Center, University of Shanghai for Science and Technology, Shanghai 200093, China
[2]Faculty of Physics and International Laser Center, Lomonosov Moscow State University, Moscow 119991, Russia
[3]IMEP-LAHC, UMR CNRS 5130, Université Savoie Mont-Blanc, Campus scientifique, 73376 Le Bourget du Lac Cedex, France
[4]Budker Institute of Nuclear Physics, Novosibirsk 630090, Russia
[5]Novosibirsk State University, Novosibirsk 630090, Russia
[6]Institute on Laser and Information Technologies–Branch of the Federal Scientific Research Centre "Crystallography and Photonics" of Russian Academy of Sciences, Svyatoozerskaya 1, Shatura 140700, Russia
[7]e-mail: ymzhu@usst.edu.cn
[8]e-mail: ashkurinov@physics.msu.ru

Received 8 February 2019; revised 30 March 2019; accepted 10 April 2019; posted 11 April 2019 (Doc. ID 359813); published 28 May 2019

We present the results of research carried out for the first time, to the best of our knowledge, on the generation of terahertz radiation under the action of "single-color" and "dual-color" high-power femtosecond laser pulses on liquefied gas–liquid nitrogen. Our experimental results supported by careful theoretical interpretation showed clearly that under femtosecond laser radiation, liquid and air emit terahertz waves in a very different way. We assumed that the mobility of ions and electrons in liquid can play an essential role, forming a quasi-static electric field by means of ambipolar diffusion mechanism.

https://doi.org/10.1364/PRJ.7.000678

1. INTRODUCTION

Femtosecond laser pulses that are focused into a gaseous medium can be a source of terahertz pulse radiation of fairly high intensity and spectral width [1]. In spite of the obvious uniformity of the physical nature of the generation of terahertz radiation in gaseous media, it is widely accepted that such terahertz generation from an optically produced spark in the gaseous medium involves two mechanisms. In the first mechanism, free electrons that are created in the medium through photoionization produce a pulse transient photocurrent that can radiate terahertz waves [2–4]. In the second mechanism, as proposed in Ref. [5], the nonlinearity of the plasma [6] that arises from the contributions of both bound and free electrons can also be a source of terahertz radiation. In one of our earlier works [7] we demonstrated that the contributions to the total terahertz signal of these two mechanisms sum up effectively and have two different frequency characteristics.

Terahertz gas photonics studies two experimental schemes: a "single-color" scheme, when only one femtosecond pulse at the frequency ω is used for the conversion into terahertz radiation, and a "dual-color" scheme, when two waves at frequencies ω and 2ω interact to generate the terahertz pulse. It is considered that these two schemes use "transient photocurrent" and "nonlinear contributions" into the sum terahertz signal in a different way. Recently [8,9], Zhang and his team have suggested using liquid as a source of terahertz radiation. They also suggested using an optical breakdown in water to generate terahertz waves. Being a polar liquid, water has considerable absorption in the terahertz frequency range [10], and thus the authors of Refs. [8,9] used very thin water films of a few-hundred-micrometer thickness in their experimental works. Differences between gas and liquid allow us to assume that the mechanisms of the terahertz radiation should be different as well. First, after ionization, in comparison to gas, free electrons in liquids exhibit a very small free path length, and thus the contribution of the free electrons' current surge decreases, as described in Ref. [2]. On the other hand, the nonlinear contribution to the terahertz signal in liquids should be much bigger than in gases [11], because the nonlinear susceptibility, for instance $\chi^{(3)}$, is 3 orders higher. The essential role of nonlinearity of the medium into the generation of a terahertz signal in liquids is indirectly confirmed in Ref. [12]. Very recently the nature of terahertz radiation in water in the dual-color interaction was explained by the effect of the nonlinear ponderomotive force that acts on the free electron movement [13], and that induces a nonlinear dipole aligned along the direction of the pumping laser beam in the liquid. The origin of terahertz radiation from optical breakdown in liquids and its possible explanations are still not completely clear and demanding additional work to be validated or explained.

In the present paper we study terahertz generation from a photoinduced plasma in liquid nitrogen (LN). We chose LN

instead of water because, besides exhibiting 3rd-order nonlinearity [14], this nonpolar liquid shows weak-up-to-moderate absorption in the visible and terahertz frequency ranges; nevertheless, this attenuation seems to shift the terahertz spectrum generated in LN to the low-frequency range. The same effect was also reported in Ref. [8]. As compared to nitrogen gas in similar conditions, the shape of the absorption spectrum of LN in the terahertz frequency range is wider with larger absorption at higher frequencies [15]. The LN absorption line is located at 1.5 terahertz, and its absorption coefficient is around 0.95 cm^{-1}. A fairly good transparency of LN in terahertz, visible, and NIR ranges enabled us to build up an experimental setup with a cuvette of the original design and rather long laser beam waist. Here we report on terahertz generation from the plasma induced in LN by two successive lasers' pulses versus the time delay between the pulses and also when LN is excited by the laser pulses at the fundamental and second-harmonic frequencies. These signals are compared to the ones generated in air. In the present paper we analyze the observed effects and interpret them, and we discuss how to increase the effectiveness of the "laser-to-terahertz" conversion.

2. EXPERIMENTAL SECTION

A. Experimental Setup

In this experimental work we use a femtosecond laser system that includes a Ti:sapphire Mira 900 oscillator and a regenerative amplifier Legend Elite Duo, both manufactured by Coherent, Inc. The system delivers pulses at 1 kHz repetition rate, whose central wavelength is 800 nm, duration is 90 fs, and energy is up to 8.5 mJ. The energy of the laser pulses is controlled by an attenuator assembled on the base of a $\lambda/2$ phase plate mounted in a rotating holder, paired with a thin polarization plate (Brewster TFP) installed in the laser beam.

The experimental setup is shown in Fig. 1. Experimental geometry is partly similar to the one in our previous work [11]. The Michelson-type interferometer creates two laser pulses and the time delay between these two pulses is varied by changing the optical path length of one arm of the interferometer (denoted ARM1 in Fig. 1) with a computer-driven motorized translation stage. At the output of the interferometer, the two pulses propagate approximately along the same axis and then

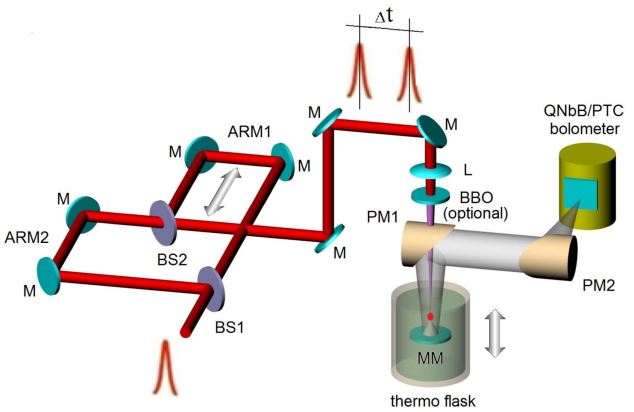

Fig. 1. Experimental setup. M–dielectric mirror; MM–metallic mirror; BS–beam splitter; $\lambda/2$–half-wave phase plate; L–lens; PM–off-axis parabolic mirror; BBO–β-barium borate crystal.

are focused into the medium under study. To decrease the variability of measurements multiple averaging is applied when acquiring a generated terahertz signal, which helps in suppressing possible phase jitter between the two interacting laser pulses due to air disturbance during their propagation through different arms of the Michelson-type interferometer. So, the jitter value of the total laser electric field is effectively averaged, and good repeatability of the measured data is provided. With the help of a set of dielectric mirrors, the two laser pulses are directed downward above or below the free surface of LN in a thermoflask. The elevation of the LN-free surface is maintained at a constant value in our experiment, at the level of the upper edge of the thermoflask. The flask is fixed to a manual translation stage, allowing it to be lifted up and down, thereby providing the controlling of the position of the sample surface in relation to the laser beam waist in vertical direction. On its way down to the sample, the laser beam passes through a lens L whose focal length is $F = 10$ cm and then through a hole in an off-axis parabolic mirror denoted as PM1 in Fig. 1; finally, it is focused either just over the liquid (i.e., in air) or inside it. The PM1 has a 50-mm focal length, a 25.4-mm diameter, and an off-axis angle of 90°. In this work, we generate terahertz waves from photoinduced plasma with both a single-color scheme (i.e., a $\omega - \omega + 0$ nonlinear interaction) and a dual-color scheme ($\omega + \omega - 2\omega$ interaction). In this latter experiment, a 300 μm β-barium borate (BBO) crystal is placed on the way of the laser beam after lens L, and here again, the focus location can be adjusted above or below the surface of the sample. A flat metallic mirror MM positioned 0.8 cm below the focus point reflects the forward-generated terahertz radiation toward the PM1. A hole of 1-mm diameter at the center of the MM prevents the destruction of this mirror by the powerful laser beam.

Terahertz radiation collimated by the PM1 is directed to a second parabolic mirror PM2 (with a focal length of 150 mm, a diameter of 50.8 mm, and an off-axis angle of 90°), which focuses it on a bolometer detector QNbB/PTC manufactured by QMC Instruments, Ltd. The QNbB/PTC bolometer system comprises a mechanically cooled cryostat into which a niobium transition edge superconducting bolometer is mounted. Low-pass blocking filters are used in the QNbB/PTC bolometer to reject unwanted higher frequencies. In our experiments, the upper frequency of the spectra of the recorded signals is limited to about 6 THz by the absorption of a Teflon filter installed in front of the detection system. It should be noted that the bolometer supplies us with the time-integrated terahertz energy.

Here we should make some comments related to the geometrical parameters of the collection scheme of the generated terahertz radiation. First, the hole in the MM passes not only the pumping laser beam but also the terahertz one generated in the axial direction within a solid angle of 5.7°. Then the maximum value of the solid angle of collection of the terahertz radiation, which is limited by the pair of PM1 and PM2, could be estimated as 28.1°. Thus, the terahertz collection system used in our experiments effectively collects radiation generated into the axial cone between the solid angles of 5.7° and 28.1°.

LN used in our experiments was obtained by the help of an ordinary membrane system of nitrogen separation from compressed air. The system provides nitrogen purity of around 98%.

B. Time-Resolved Measurements

We carry out a series of experimental investigations on the dependence of the terahertz yield from LN versus the time delay Δt between the two laser pulses when focusing them at different depths below or above the LN surface. We also compare the terahertz signal from LN to the one generated in air under the same excitation conditions. The experimental results are presented in Fig. 2. The time delay Δt is set equal to 0 when the two laser pulses hit the sample simultaneously; a negative value of Δt means that the laser pulse which passes through ARM1 arrives at the sample after the pulse which comes from ARM2. In this work, the polarizations of the two consecutive laser pulses are the same. The energies of the laser pulses from ARM1 and ARM2 are, respectively, 1.25 mJ and 1.20 mJ. We perform two series of experiments: in the first series, the two successive pulses exhibit the same central optical frequency ω (single-color scheme), i.e., a $\omega - \omega$ nonlinear interaction; in the second series, a nonlinear crystal, located in the path of the beams just after the focusing lens L, supplies the second harmonic of the laser frequency and allows us to perform a $\omega + \omega - 2\omega$ interaction (dual-color scheme).

The dependencies of the terahertz signal generated in LN shown in Figs. 2(a) and 2(b) were measured when the focus of optical radiation was located at a depth of 4.5 mm below the LN surface. We should note that the terahertz yield curves, measured for the cases of positioning of the laser focus at smaller or greater depths, behaved similarly, and here the results obtained only for the case when the laser pulses focus was at the depth of 4.5 mm are shown.

In Fig. 2(a), the signals are generated both in LN and in air using the single-color scheme. We see that the shapes of the recorded curves change significantly when the laser focus goes from LN to air: the signal from air exhibits a strong peak at $\Delta t = 0$, while the one from LN shows a pronounced depression with a minimum at $\Delta t = 0$. In addition, the depression is wider than the peak: the full width at half-maximum (FWHM) of the peak (terahertz signal generated in air) is about 150 fs. The FWHM value of the depression (signal generated in LN) increases up to ≈1.8 ps. In addition, as seen in Fig. 2, the terahertz yield from LN returns to its maximum plateau level when the time delay between the laser pulses is longer than ∼2–4 picoseconds; i.e., it exceeds the duration of each laser pulse by several times.

In Fig. 2(b), we plot the terahertz curves from LN in the case of the single-color (black circles) and dual-color (blue circles) excitation schemes. In the latter case, the intensity of the terahertz radiation is 1.5 orders of magnitude greater than in the single-color one, and the FWHM of the peak at $\Delta t \approx 0$ is close to the one observed for terahertz generation in air [Fig. 2(c)].

C. Terahertz Power Measurements

The position of the focal spot of the laser beam relative to the LN surface has a strong effect on the terahertz pulse energy.

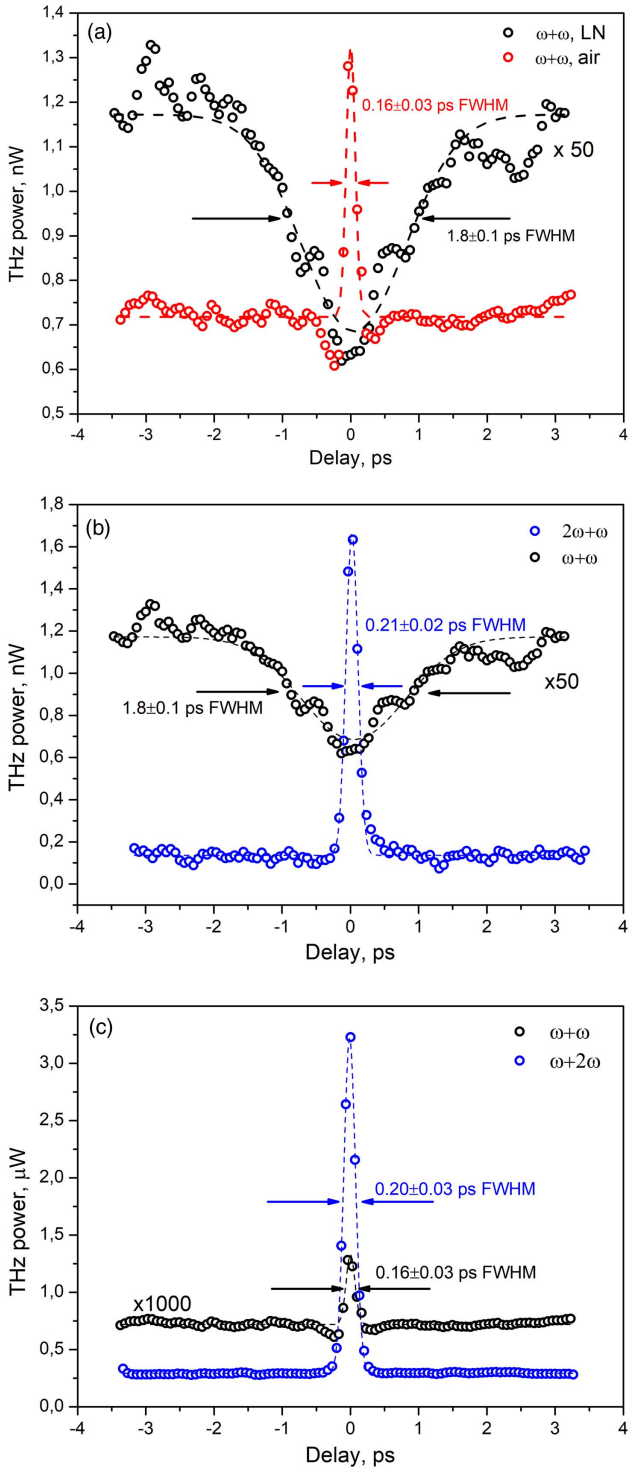

Fig. 2. Terahertz yield via the time delay between the laser pulses. (a) Single-color interaction in air (red circles) and in LN (black circles). (b) LN: single-color (black) and dual-color (blue) schemes. (c) Air: single-color (black) and dual-color (blue) schemes. Each curve is fitted by a simple Gaussian peak to get FWHM value.

Throughout this paper, we use also the term "beam waist" as the plasma is produced only nearby the focus of the laser. In this work, we focus the laser beam with a lens of focal length $F = 10$ cm, for which the Rayleigh length corresponding to a

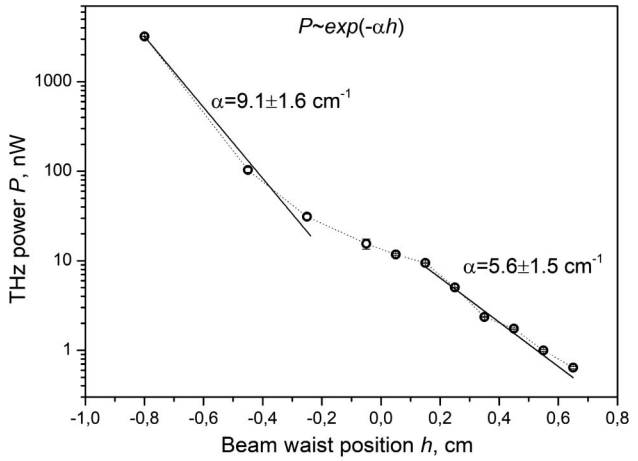

Fig. 3. Dependence of terahertz pulse power on the beam waist position h in relation to the surface level of LN. Zero position of the abscissa axis corresponds to the surface of LN. Peak amplitude of the terahertz pulse power is measured in two beams' dual-color regime [blue dots in Fig. 2(b)].

Gaussian waist of 16-μm diameter can be estimated as 500 μm [16]. It means that the focused beam in air and especially in LN is very well localized, and indeed, we did not observe visually the formation of an extended filament.

Figure 3 shows the terahertz pulse energy versus the position h of the focus in relation to the LN surface. The beam waist positions below zero (where zero is the level of LN) correspond to terahertz generation in air (above the LN surface), while the positive beam waist positions correspond to terahertz generation in the LN (see experimental setup in Fig. 1). In both cases there is an attenuation of the generated terahertz signal as it is propagated in LN. If we neglect optical losses in LN and take into consideration the attenuation of terahertz radiation in it, the experimental dependence would look like two exponential decays with a smoothed shift near the surface of LN. This is due to the relationship between beam waist position h and the total terahertz propagation path l in LN: for $h < 0, l = 2(h + 0.8)$, where 0.8 cm is the distance between the flat mirror and the focal point (see Fig. 1). For $h > 0, l = h + 1.6$, similar calculations will lead to the value of the exponent, which is two times smaller than for $h < 0$. This is what is practically observed in Fig. 3. Using these data, one can calculate the extinction coefficient for terahertz radiation in LN. On the basis of the abovementioned calculations, we estimate the absorption coefficient for terahertz radiation in LN to be approximately 4.5 cm^{-1}. This value is higher than the value 0.95 cm^{-1} in Ref. [15]. We suppose that it is due to heating or to some nonlinear process because of the huge optical and terahertz peak powers. The shift in the experimental dependence curve at the LN surface level could be attributed to the different efficiency of laser-terahertz conversion in air and in LN. Moreover, the contributions of additional nonlinearity of the LN surface and the reflection (and scattering) losses of femtosecond laser radiation at the LN surface have to be considered as well. To summarize, the experimental data plotted in Fig. 3 exhibit both a change of slope (power law

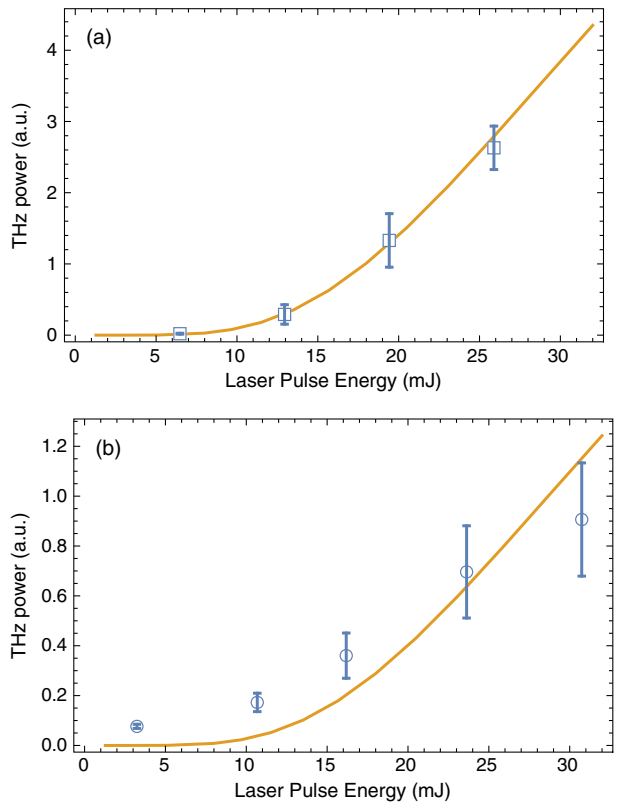

Fig. 4. Radiated terahertz energy versus laser pulse energy: solid squares with error bars show experimental data, and solid line stands for theoretical model. (a) Focal spot located in the air; (b) focal spot located in the liquid nitrogen.

of the terahertz signal versus laser power) and in the generation efficiency.

We also measured the dependencies of the generated terahertz power on laser pulse energy for the case of one beam dual-color excitation scheme with laser energy up to 30 mJ per pulse. Experimental results for gaseous and liquid media are presented in Figs. 4(a) and 4(b) correspondingly with symbols.

3. THEORETICAL MODELS AND DISCUSSION

A. Asymmetric Ionization

We employ the model of asymmetric ionization, also known as the model of transient photocurrent. This model was proposed by Kim *et al.* [2,17]. These authors (see also our paper [3]) suggested that asymmetric field ionization by a dual-color laser pulse causes the formation of a rectified current, which is sometimes called the residual current density (see, e.g., Ref. [18]). The model is routinely applied to the interaction of two linearly polarized harmonics. We first write down the dual-color laser field as

$$E_x = E_\omega \cos(\omega t) + E_{2\omega} \cos(2\omega t + \phi),$$
$$E_y = 0, \qquad E_z = 0, \tag{1}$$

where E_ω and $E_{2\omega}$ are the amplitudes of the first and second harmonics, respectively. Here, the z axis corresponds to the direction of propagation of the laser beam, while x and y axes are

perpendicular to this direction. Both laser fields are polarized along x.

Following Ref. [18], we assume that the density n_e of free electrons in the focal spot region is governed by the equation

$$\frac{\partial n_e}{\partial t} = (n_f - n_e)w(E), \tag{2}$$

where n_f denotes the density concentration of a gas or a liquid, $w(E)$ is the probability of the tunnel and barrier-suppression ionization, and E is the total field amplitude. As suggested in Ref. [19], the probability can be evaluated as

$$w(E) = \frac{4\omega_a E_a}{E}\exp\left(-\frac{2E_a}{3E} - \frac{12E}{E_a}\right), \tag{3}$$

where $\omega_a = 4.13 \times 10^{16}$ s^{-1} and $E_a = 5.14$ GV/cm are the atomic units of the frequency and electric field, respectively. Note that the model Eq. (3) was derived using a semi-classical approach for the ionization by a static electric field, and therefore the value of ω_a might have been greatly overestimated (see below).

If we neglect collisions, the equation of motion of a free electron simply writes

$$\frac{d\vec{v}}{dt} = \frac{e}{m}\vec{E}. \tag{4}$$

By integrating Eq. (4) for a free electron generated at time t_0 with zero initial speed [20], we evaluate the drift component $\vec{V}$ of the velocity $\vec{v}$, which is defined as the average value of $\vec{v}$ over the period $2\pi/\omega$. It has only an x component:

$$V_x(t_0) = \frac{v_\omega}{2}[-\mu \sin(2\omega t_0 + \phi) - 2\sin(\omega t_0)]. \tag{5}$$

Here $v_\omega = eE_\omega/m\omega$, and $\mu = E_{2\omega}/E_\omega$. The production of the rectified current is then governed by the following equation [3]:

$$\frac{\partial}{\partial t}\vec{J}(t) = e\vec{V}(t)\frac{\partial}{\partial t}n_e(t) \approx e\vec{V}(t)n_f w[E(t)], \tag{6}$$

as long as $n_e \ll n_f$. If the probability of generating free electrons is the same whatever time t_0, then the rectified current is zero, since the mean value of the drift velocity in Eq. (5), calculated over t_0, is zero.

The rectified current is also zero if there is no second harmonic field, i.e., $E_{2\omega} = 0$. Indeed, in this case, the magnitude of the laser field is $E = E_\omega$, and it does not vary with time t. Similarly, in accordance with Eq. (3), the probability of the production of free electrons does not depend on time t, whereas the drift velocity of these electrons changes its sign every half-period. This leads to the cancellation of the rectified current. The addition of a second harmonic destroys this symmetry and makes it possible to produce a nonzero current.

Finally, we compute the rectified current density J as a function of the square $E^2 = E_\omega^2 + E_{2\omega}^2$ of the dual-color laser pulse amplitude. This allows us to fit the measured dependence of the total energy of terahertz radiation on the laser pulse energy. As seen in Fig. 4(a), the model is in a very good agreement with the experimental data when terahertz radiation is produced in air. For terahertz generation in LN, the model reflects the tendency of the experimental records, but the fit is not as good as for generation in air [Fig. 4(b)]. We suggest that the difference between experimental and theoretical data in Fig. 4(b) may be attributed to the huge reduction of the mean free path length of electrons in LN as compared to that in air. This reduction leads to a decrease of the efficiency of terahertz generation process. Besides, we assume that the change in the efficiency of the terahertz generation is also affected by the ambipolar DC field formed in the focal spot in LN under the action of the laser pulse. You will find the description of this effect in the next section.

B. Ambipolar Diffusion of Electrons in a Liquid

We first estimate the percentage of ionized molecules in the photoinduced plasma. Assuming that the total energy, when both laser pulses strike the sample, is $W = 2$ mJ, and the ionization cost is $P = 100$ eV per electron [21], the total number of free electrons, born upon complete absorption of the laser pulse in the liquid, is estimated to be $N_e = W/P = 1.25 \times 10^{14}$. Note that this is an overestimated value, as the laser beam is not completely absorbed in LN.

The radius of the waist at the focal spot is $a = 8$ μm, and its Rayleigh length is $L = 500$ μm; thus, the electron density is estimated at the level of $n_e = N_e/\pi a^2 L = 1.2 \times 10^{21}$ cm^{-3}. Its actual value is certainly smaller; therefore, in any case it is much less than the density of the fluid $n_f = 10^{23}$ cm^{-3}. Thus, the plasma formed at the focal spot is only partially ionized. The rate of ionization ν_{ioniz} can be evaluated from the equation $n_e = \nu_{\text{ioniz}} n_f \tau$, which yields $\nu_{\text{ioniz}} = 1.4 \times 10^{12}$ s^{-1} for a pulse duration $\tau = 90$ fs. Therefore, we conclude that the actual ionization rate is many orders of magnitude smaller than the one predicted by the model of barrier-suppression ionization in a static electric field (see, e.g., Ref. [22]). Presumably, this occurs because most of the laser pulse energy serves to evaporate LN.

The electron mean free path in the plasma is given by $\lambda_e = 1/n_f\sigma$. In the first approximation, we take $\sigma = 10^{-16}$ cm^2. Such a value corresponds to an upper estimate of the cross section for scattering of an electron by an atom or of the cross section for the impact ionization of an atom by an electron (so far, we do not take into account the fact that the cross section is smaller for a high-energy electron). Then it turns out that the mean free path $\lambda_e = 0.1$ μm is many orders of magnitude smaller than the waist radius of the focal spot (that is why the refinement of the cross section is not very significant). Thus, we conclude that the motion of free electrons in a liquid has a character of diffusion.

The diffusion tends to smooth out the initial inhomogeneous spatial distribution of electrons. In a plasma, even weakly ionized, the diffusion is accompanied by the appearance of the DC electric field, which is directed along the radius of the waist and tends to equalize the radial fluxes of electrons and ions to support the quasi-neutrality of the focal spot (see Fig. 5).

Very recently, Mori *et al.* [23] have reported on an experiment rather similar to ours but in which plasma is created in a cloud of argon clusters. They suggest that the ions emitted from the clusters, which are Coulomb-exploded by the first laser pulse, form a positively charged ion cloud that acts as a bias. In the plasma channel created by the second pulse a transverse current [24] or dipole moment [25] is excited, which leads to

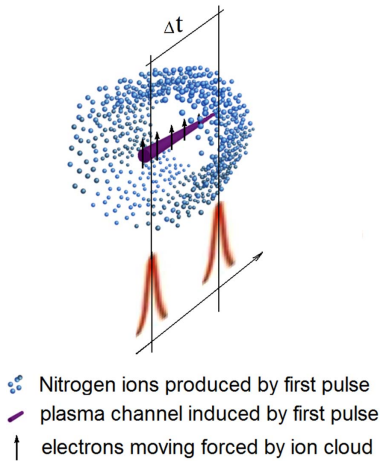

Fig. 5. Diagram of terahertz generation from "liquid" plasma under irradiation by a double-pulse beam.

the emission of electromagnetic waves just like terahertz wave generation in a DC field.

In our experiments with LN, we also assume that the laser pulse results in the separation of ions and electrons, forming the ambipolar field. This field has a cylinder symmetry, and for further modelling of nonlinear optical processes, it has a DC character. The second laser pulse, which is delayed in relation to the first one, propagates in this DC field. In the case of a single-color scheme, we can neglect the dispersion broadening in the medium. Thus, we consider the interaction of the femtosecond laser pulse with this DC field to be effective. In our case, we used the experimental scheme when laser pulses propagated following the same trajectory twice being reflected backward, thus intensifying the role of the DC field in nonlinear interaction.

The estimated degree of ionization is so small that collisions of charged particles with each other can be neglected in comparison to their collisions with neutral atoms. Even under these conditions, as Walter Schottky explained [26], the diffusion of one kind of charged particles, for example electrons, affects the diffusion of another sort of charged particles, i.e., ions. This occurs due to the so-called ambipolar electric field (see, e.g., Ref. [27], Eq. (25.14)])

$$\vec{E} = \frac{T}{e}\frac{\vec{\nabla} n_e}{n_e}. \tag{7}$$

This field remains near the laser beam waist as long as the plasma carrier density is not homogeneous. Assuming a rough estimation $T = 100$ eV and $a = 8$ μm (however, the cloud expands as shown in Fig. 5), Eq. (7) yields $E > 20$ kV/cm, which exceeds the maximal external electrostatic field applied to the laser spot in the experiments described in Ref. [24]. These experiments have demonstrated a strong enhancement of the terahertz radiation when an external DC electric field of such an intensity is applied at the laser focus location. Therefore, we suggest that the ambipolar field might also serve as a booster of the terahertz radiation magnitude. Note, however, that the qualitative estimations based on Eq. (7) can be seriously hampered by the formation of gas bubbles at the focal spot location.

C. Four-Wave-Mixing Process

Because of the ambipolar field, the terahertz generation by the second laser pulse should be treated in the framework of the four-wave-mixing (FWM) phenomena. The polarization properties of the terahertz radiation are defined by the symmetry properties of the plasma and the contributions of N_2 molecular motions. In the framework of the FWM theory (see, e.g., Ref. [28]), the expression of the 3rd-order nonlinear polarization is

$$P_i^{(3)}(\omega_q) = \chi_{ijkl}^{(3)}(\omega_q;\omega_m,\omega_n,\omega_r)E_j(\omega_m)E_k(\omega_n)E_l(\omega_r), \tag{8}$$

where $\omega_q = \omega_m + \omega_n + \omega_r$, and $\vec{E}(\omega_p)$ is the complex amplitude of the wave at the frequency ω_p $(p = q, m, n, r)$. In an isotropic medium such as air or LN, the nonlinear susceptibility tensor $\chi_{ijkl}^{(3)}$ depends only on three independent coefficients $\mathbb{A}$, $\mathbb{B}$, and $\mathbb{C}$, which are functions of the involved frequencies:

$$\chi_{ijkl}^{(3)} = \mathbb{A}\delta_{ij}\delta_{kl} + \mathbb{B}\delta_{ik}\delta_{jl} + \mathbb{C}\delta_{il}\delta_{jk}. \tag{9}$$

δ_{ij} is the Kronecker symbol. The classical theory of nonlinear polarization [28] reveals that these three coefficients are equal, and their expression is

$$\mathbb{A} = \mathbb{B} = \mathbb{C} = \sum_{(mnr)} \frac{b n_f e^4/m_e^3}{G(\omega_q)G(\omega_m)G(\omega_n)G(\omega_r)}, \tag{10}$$

where $G(\omega) = \omega_0^2 - \omega^2 - 2i\gamma\omega$, ω_0 is the atomic frequency, γ is the damping rate due to energy relaxation (through vibration of molecules, phonons, etc.), n_f is the density of the medium, m_e is the mass of the electron, and the summation goes over frequencies ω_m, ω_n, and ω_r such that $\omega_q = \omega_m + \omega_n + \omega_r$. The phenomenological parameter b is of the order of $b \simeq \omega_0^2/d^2$, where d is the atomic dimension. Using this expression for b, Boyd [28] estimated the expression of nonlinear susceptibility as

$$\chi^{(3)} \simeq \frac{e^4 n_f}{m_e^3 \omega_0^6 d^2}, \tag{11}$$

where n_f is $\sim 1/d^3$ for a fluid.

Therefore, the 3rd-order nonlinear susceptibility is proportional to the medium density, and, consequently, it is many orders of magnitude smaller in air or gaseous nitrogen than in LN. Note also that for a molecular nonpolar liquid such as LN, the molecular frequency ω_0 is much lower than the laser frequency ($\omega_0 \sim 1$ THz), and hence the nonlinear susceptibility is determined mainly by the laser-related frequencies ω_m, ω_n, and ω_r. This observation leads to the following important conclusion. If $\omega_0 \ll \omega$, a relatively low ambipolar DC field $\vec{E}(0)$ contributes to the 3rd-order polarization at the same level as a much greater laser field at doubled frequency (2ω).

The generation of terahertz radiation at a frequency Ω (much lower than the central frequency ω of the laser radiation) is completely determined by Eq. (8) in which $\omega_q \sim \Omega$. Here we assume that the spectral widths of the laser lines ω_m, ω_n, ω_r are of the order of $\Omega \sim 2\pi/\tau$, where τ is the laser pulse duration.

When short laser pulses with central frequencies ω, 2ω interact with each other and ambipolar field $\vec{E}(0)$ in a medium with cubic nonlinearity, we input the frequencies ω, 2ω and 0

into Eq. (8). Thus, the polarization $\vec{P}(\Omega)$ takes the following symbolic form:

$$P_i^{(3)}(\Omega) = \chi_{ijkl}^{(3)}(\Omega; -2\omega, \omega, \omega)E_j^*(2\omega)E_k(\omega)E_l(\omega) + \chi_{ijkl}^{(3)}(\Omega; 0, \omega, -\omega)E_j(0)E_k(\omega)E_l^*(\omega) + \chi_{ijkl}^{(3)}(\Omega; 0, 2\omega, -2\omega)E_j(0)E_k(2\omega)E_l^*(2\omega), \quad (12)$$

where, for the sake of simplicity, we drop integration over natural spectral widths of the laser pulses at the fundamental and double frequencies.

The ambipolar field contribution [last two terms in Eq. (12)] to the nonlinear polarization proves to be much stronger than the FWM contribution of the laser pulses at frequencies ω and 2ω [first term in Eq. (12)]. Indeed, we derive from Eq. (10) the following relation for the coefficients in Eq. (12):

$$\frac{\chi_{ijkl}^{(3)}(\Omega, \Omega, n\omega, -n\omega)}{\chi_{ijkl}^{(3)}(\Omega, -2\omega, \omega, \omega)} \sim \frac{n\omega^2}{\Omega^2} \gg 1, \quad (13)$$

with either $n = 1$ or $n = 2$.

Our tentative model can also explain experimental observations reported in the literature (see, for example, Refs. [24,29]). In these publications, it is demonstrated that an external static field of the order of a few kV/cm causes an increase of the terahertz signal radiated by the plasma, approximately as noticeable as the enhancement due to the addition of a second-harmonic laser pulse, although the amplitude of the 2ω laser field is by several orders of magnitude greater than the one of the static field. In the present experiment, we suggest that the ambipolar field in the laser focus region in the liquid causes an equally strong effect. However, we note that, in the dual-color scheme, the mechanism of transient photocurrent discussed previously yields even larger terahertz radiation as seen from Fig. 2. Let us also notice that the DC field destroys the symmetry of the total electric field and therefore can contribute to asymmetric ionization. However, this effect seems to be much weaker than the effect of adding second harmonics on asymmetry ionization.

D. Phenomenological Explanation of the Depression in the Single-Color Experimental Record

The terahertz waveform [Fig. 2(a)] from the plasma in LN, recorded in the single-color scheme, shows a depression when the two successive laser pulses overlap, while a similar waveform from air exhibits a strong positive peak. Let us try here to explain these behaviors.

The first pulse creates plasma in LN and simultaneously it generates a terahertz signal through the 2nd-order nonlinear effect ($\omega - \omega = 0$). Then an ambipolar field appears due to the Coulomb explosion (diffusion of the free electrons toward the outer region of the plasma, while nitrogen ions may be considered as immobile). The second pulse arrives in the medium with a delay time Δt [see Fig. 6(a)]. Depending on the value of Δt, one can separate five different regimes of terahertz generation by the second pulse.

- When Δt is larger than the plasma lifetime, the second pulse excites LN that has returned to its fundamental state. Both first and second pulses generate equal terahertz signals, which simply add when recording the integrated terahertz energy.
- When Δt is shorter than the plasma lifetime but still longer than the ambipolar field lifetime, the plasma is neutral. The second pulse generates a terahertz signal through the 2nd-order effect ($\omega - \omega = 0$) but in the plasma instead of in LN at equilibrium. It could be expected that the terahertz signal is bigger than from LN, because of the contributions of both bound and free electrons, but the difference should be not so big.
- At shorter delay times, the ambipolar field still exists in the plasma. The main source of terahertz generation is the 3rd-order nonlinearity, involving the ambipolar field through the $\omega - \omega + 0 = 0$ interaction. Let us notice that terahertz generation through 2nd-order effect $\omega - \omega = 0$ still occurs simultaneously in the plasma. But, even if 3rd-order effects are less efficient than 2nd-order ones, here the 3rd-order one is predominant, because the plasma is almost centrosymmetric.
- At delay times shorter than the laser pulse duration, both pulses probe the same medium through a 2nd-order effect, as

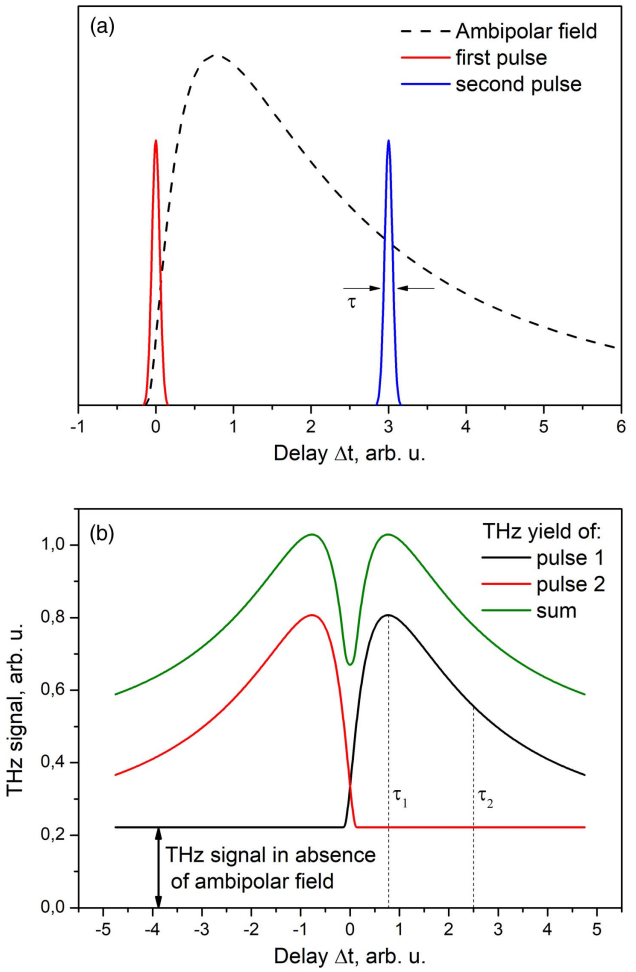

Fig. 6. Schematic representation of the ambipolar field effect on the terahertz yield. (a) Field formation by the first pulse and probing by the second one; (b) total terahertz yield from two pulses with variable delay. τ corresponds to the optical pulse duration, while τ_1 and τ_2 correspond to the characteristic times of ambipolar field formation and decay.

the ambipolar field had not enough time to be established. The terahertz signal is thus weaker than when the ambipolar field exists. Nevertheless, it is bigger (double) than at very long delay times, because the total laser field in LN is twice the one of a single laser pulse.

All these stages are schematically depicted in Fig. 6. When the recording time window is shorter than the ambipolar field lifetime, the decrease at longer times is not observed. It is what is seen in Fig. 2(a). Thus, we deduce that the ambipolar lifetime is longer than a few ps. According to our explanation, the temporal width of the depression at delay times $\Delta t \sim 0$ corresponds to the requested time for the ambipolar field to be fully established, i.e., when the Coulomb force due to this field exactly compensates for the Coulomb explosion. Here the temporal width at HWFM of the depression is about 2 ps.

The terahertz signal generated in the air plasma is much stronger than in LN, even if the density of air, and thus the number of photocreated free electrons, are smaller than in LN. Moreover, the signal exhibits a peak instead of a depression at $\Delta t \approx 0$. This positive peak corresponds to the autocorrelation trace of the laser pulses through a nonlinear effect. Following our previous explanation, the strong signal from air is due to the $\omega - \omega + 0 = 0$ interaction, which implies that the ambipolar field appears almost instantaneously in air. Also, the ambipolar field magnitude should be bigger than in LN. This could be explained by a faster and easier diffusion of the free electrons, which encounter less velocity of a damping effect (like collision or other polarization effects) in air.

4. CONCLUSION

In this paper we present the first observation of terahertz generation by photoexcitation of a liquefied gas. We use a time-resolved double pulse excitation scheme, in which the second pulse probes the liquid after excitation by the first pulse. We employ single-color and dual-color excitation schemes, and compare results obtained when terahertz generation appeared from the plasma created by the optical breakdown in air and from LN. We demonstrate that both the ionization of the medium and its nonlinear susceptibility play a considerable role in the generation of terahertz radiation in LN. We assume that the mobility of ions and electrons in liquid can play an essential role, forming a quasi-static electric field by means of an ambipolar diffusion mechanism. This quasi-stationary field permits the terahertz generation through a 3rd-order nonlinear effect, which is stronger than 2nd-order effects in quasi-centrosymmetric media-like plasmas. We will pursue this work by studying the polarization dependence of this terahertz generation in LN, with the view of validating our tentative explanation of the phenomenon and determining the main coefficients of the $\chi^{(3)}$ tensor. This should allow us to propose experimental schemes to optimize the efficiency of terahertz generation in gas and liquid.

Funding. Russian Foundation for Basic Research (RFBR) (17-02-01217, 18-29-20104, 18-52-16016); Major National Development Project of Scientific Instrument and Equipment, China (2016YFF0100503); National Natural Science Foundation of China (NSFC) (61722111); 111 Project, China (D18014); International Joint Lab Program supported by Science and Technology Commission of Shanghai Municipality (STCSM) (17590750300).

Acknowledgment. We would like to thank the Russian-French International Research Network (IRN) FIR-LAB. We thank X.-C. Zhang and A. Rukhadze for fruitful discussions. The authors thank A. Bunkin, I. Ozheredov, and S. Pershin for their continuous support. This work was partially supported by the Ministry of Science and Higher Education within the State assignment of the Federal Scientific Research Centre "Crystallography and Photonics" of the Russian Academy of Sciences.

REFERENCES

1. X.-C. Zhang, A. Shkurinov, and Y. Zhang, "Extreme terahertz science," Nat. Photonics **11**, 16–18 (2017).
2. K. Y. Kim, J. H. Glownia, A. J. Taylor, and G. Rodriguez, "Terahertz emission from ultrafast ionizing air in symmetry-broken laser fields," Opt. Express **15**, 4577–4584 (2007).
3. A. V. Balakin, A. V. Borodin, I. A. Kotelnikov, and A. P. Shkurinov, "Terahertz emission from a femtosecond laser focus in a two-color scheme," J. Opt. Soc. Am. B **27**, 16–26 (2010).
4. M. Li, W. Li, Y. Shi, P. Lu, H. Pan, and H. Zeng, "Verification of the physical mechanism of THz generation by dual-color ultrashort laser pulses," Appl. Phys. Lett. **101**, 161104 (2012).
5. D. J. Cook and R. M. Hochstrasser, "Intense terahertz pulses by four-wave rectification in air," Opt. Lett. **25**, 1210–1212 (2000).
6. N. Bloembergen and Y. R. Shen, "Optical nonlinearities in a plasma," Phys. Rev. **145**, 390 (1966).
7. A. V. Borodin, N. A. Panov, O. G. Kosareva, V. A. Andreeva, M. N. Esaulkov, V. A. Makarov, A. P. Shkurinov, S. L. Chin, and X.-C. Zhang, "Transformation of terahertz spectra emitted from dual-frequency femtosecond pulse interaction in gases," Opt. Lett. **38**, 1906–1908 (2013).
8. Q. Jin, Y. E, K. Williams, J. Dai, and X.-C. Zhang, "Observation of broadband terahertz wave generation from liquid water," Appl. Phys. Lett. **111**, 071103 (2017).
9. Q. Jin, J. Dai, Y. E, and X.-C. Zhang, "Terahertz wave emission from a liquid water film under the excitation of asymmetric optical fields," Appl. Phys. Lett. **113**, 261101 (2018).
10. T. Wang, P. Klarskov, and P. U. Jepsen, "Ultrabroadband THz time-domain spectroscopy of a free-flowing water film," IEEE Trans. Terahertz Sci. Technol. **4**, 425–431 (2014).
11. A. V. Balakin, S. V. Garnov, V. A. Makarov, N. A. Kuzechkin, P. A. Obraztsov, P. M. Solyankin, A. P. Shkurinov, and Y. Zhu, ""Terhune-like" transformation of the terahertz polarization ellipse "mutually induced" by three-wave joint propagation in liquid," Opt. Lett. **43**, 4406–4409 (2018).
12. I. Dey, K. Jana, V. Y. Fedorov, A. D. Koulouklidis, A. Mondal, M. Shaikh, D. Sarkar, A. D. Lad, S. Tzortzakis, A. Couairon, and G. R. Kumar, "Highly efficient broadband terahertz generation from ultrashort laser filamentation in liquids," Nat. Commun. **8**, 1184 (2017).
13. Y. E, Q. Jin, A. Tcypkin, and X.-C. Zhang, "Terahertz wave generation from liquid water films via laser-induced breakdown," Appl. Phys. Lett. **113**, 181103 (2018).
14. H. Kildal and S. R. J. Brueck, "Orientational and electronic contributions to the third order susceptibilities of cryogenic liquids," J. Chem. Phys. **73**, 4851–4958 (1980).
15. J. Samios, U. Mittag, and T. Dorfmuller, "The far infrared absorption spectrum of liquid nitrogen," Molecular Physics **56**, 541–556 (1985).
16. A. Siegman, *Lasers* (University Science Books, 1986).
17. K. Y. Kim, A. J. Taylor, J. H. Glownia, and G. Rodriguez, "Coherent control of terahertz supercontinuum generation in ultrafast laser-gas interactions," Nat. Photonics **2**, 605–609 (2008).

18. N. V. Vvedenskii, A. I. Korytin, V. A. Kostin, A. A. Murzanev, A. A. Silaev, and A. N. Stepanov, "Two-color laser-plasma generation of terahertz radiation using a frequency-tunable half harmonic of a femtosecond pulse," Phys. Rev. Lett. **112**, 055004 (2014).
19. V. A. Kostin, I. D. Laryushin, A. A. Silaev, and N. V. Vvedenskii, "Ionization-induced multiwave mixing: terahertz generation with two-color laser pulses of various frequency ratios," Phys. Rev. Lett. **117**, 035003 (2016).
20. W.-M. Wang, Z.-M. Sheng, H.-C. Wu, M. Chen, C. Li, J. Zhang, and K. Mima, "Strong terahertz pulse generation by chirped laser pulses in tenuous gases," Opt. Express **16**, 16999–17006 (2008).
21. C. F. Barnett and M. F. A. Harrison, *Applied Atomic Collision Physics: Plasmas* (Academic Press, Inc., 1984), Vol. **2**.
22. A. V. Balakin, M. S. Dzhidzhoev, V. M. Gordienko, M. N. Esaulkov, I. A. Zhvaniya, K. A. Ivanov, I. A. Kotelnikov, N. A. Kuzechkin, I. A. Ozheredov, V. Y. Panchenko, A. B. Savel'ev, M. B. Smirnov, P. M. Solyankin, and A. P. Shkurinov, "Interaction of high-intensity femtosecond radiation with gas cluster beam: effect of pulse duration on joint terahertz and X-ray emission," IEEE Trans. Terahertz Sci. Technol. **7**, 70–79 (2017).
23. K. Mori, M. Hashida, T. Nagashima, D. Li, K. Teramoto, Y. Nakamiya, S. Inoue, and S. Sakabe, "Directional linearly polarized terahertz emission from argon clusters irradiated by noncollinear double-pulse beams," Appl. Phys. Lett. **111**, 241107 (2017).
24. A. Houard, Y. Liu, B. Prade, V. T. Tikhonchuk, and A. Mysyrowicz, "Strong enhancement of terahertz radiation from laser filaments in air by a static electric field," Phys. Rev. Lett. **100**, 255006 (2008).
25. N. A. Panov, O. G. Kosareva, V. A. Andreeva, A. B. Savel'ev, D. S. Uryupina, R. V. Volkov, V. A. Makarov, and A. P. Shkurinov, "Angular distribution of the terahertz radiation intensity from the plasma channel of a femtosecond filament," JETP Lett. **93**, 638–641 (2011).
26. W. Schottky, "Diffusionstheorie der positiven säule," Phys. Zeits **25**, 635 (1924).
27. L. D. Landau and E. M. Lifshitz, *Physical Kinetics: Course of Theoretical Physics* (Pergamon, 1984), Vol. **X**.
28. R. W. Boyd, *Nonlinear Optics*, 2nd ed. (Academic, 1992).
29. W.-F. Sun, Y.-S. Zhou, X.-K. Wang, and Y. Zhang, "External electric field control of THz pulse generation in ambient air," Opt. Express **16**, 16573–16580 (2008).